 doi:10.20944/preprints202008.0405.v1

Article

Temperature-dependent physical characteristics and varying heat effects on nonlocal rotating nanobeams due to dynamic load

Ahmed E. Abouelregal[1,2],* F. A. Mohammed[1,3], Mohamed V. Moustapha[1,4], and Doaa Atta[2,5]

[1]Department of Mathematics, College of Science and Arts, Jouf University, Al-Qurayyat, Saudi Arabia, [2]Department of Mathematics, Faculty of Science, Mansoura University, Mansoura 35516, Egypt, ahabogal@mans.edu.eg, [3]Department of Mathematics, South Valley University, Egypt, fawzy.noureldeen@sci.svu.edu.eg, [4]Faculty of sciences and techniques - University Alasriya of Nouakchott Nouakchott- Mauritania, mohamedvall.ouldmoustapha230@gmail.com, [5]Department of Mathematics, College of Science, Qassim University, P.O. Box 6644, Buraydah 51482, Saudi Arabia, doaaatta44@gmail.com

* Correspondence: ahabogal@mans.edu.eg

Abstract:

A theoretical nonlocal thermoelastic model for studying the effects of the thermal conductivity variability on a rotating nanobeam has been described in the present article. The theory of thermal stress is employed using the Euler–Bernoulli beam model and generalized heat conduction with phase lags. It is believed that the thermal conductivity of the current model varies linearly according to temperature. Due to variable harmonic heat, the considered nanobeam excited and was subjected to a time-varying exponential decay load. Using the Laplace transform process, the analytical solutions for displacement, deflection, thermodynamic temperature and bending moment of rotating nanobeams are provided in final forms and a numerical example has been taken to address the problem. A comparison of the stated results was displayed and additionally, the influences of non-local parameter and varying load were analyzed and examined. We also investigate how the linear changes in the temperature of physical properties can influence both the static and dynamic responses to the rotating nanobeam.

Keywords: Nonlocal nanobeam; rotation; thermoelasticity; temperature-dependent; varying load

---

1. Introduction

Mechanical thermal influences resulting from the interaction of temperature and deformation fields are of particular significance in various modern designs like high-speed aircraft, jets, gas and steam turbines, nuclear reactors and missiles. Theoretical and the study of many practical issues, including rapid heat energy supply, has gained growing attention. The conventional theory of heat conduction,

 doi:10.20944/preprints202008.0405.v1

based on the law of Fourier, takes an instant reaction to the temperature gradient and tends to a distinctive parabolic equation for temperature development.

To solve the infinite speed thermal propagation phenomena predicted by the classical thermoelasticity theory, modified generalized theories of thermoelasticity have been established. Lord and Shulman [1] suggested one of the modified generalized thermoelasticity theories that contained one relaxation time by introducing a novel law of thermal conductivity to exchange the classic Fourier law. This revised law includes the flux of heat and its partial derivative with respect to time. Among the models that have recently been very popular, the Tzou [2-4] model. In this model, Tzou introduced the dual-delay thermal heat conduction model (DPL) to include the effects of microscopic reactions into the rapid transit of the heat transfer mechanism into a microscopic formula. In the constitutive relationship between the heat flux and the temperature gradient, two different phase-lags have been introduced. There are many other suggestions that have been made to overcome the problem of unlimited speeds of heat waves predicted by the classical thermoelasticity theory can be found in [5-8].

Thermal conductivity is significant, especially when high operating temperatures are reached, in materials sciences, research and electronics, building insulation, and associated fields. The temperature has a distinctive impact on the thermal conductivity for metals and non-metals materials. The thermal conductivity of metal materials is the electric conductivity compared to absolute temperature times. With the expanding temperature, the electrical conductivity in pure metals decreases. The result, the thermal conductivity, is approximately constant along these lines. In alloys, the electric conductance change is generally smaller, so the temperature rises thermal conductivity, always relative to the temperature [9].

The smallest Electromechanical Systems area (MEMS) is quickly divided into different resistors and applications. In order to satisfy the industry requirements, new technologies have been used to produce a range of MEMS products. MEMS structures include mechanical components, e.g. small cantilevers, extensions and films that have been frequently filled with a variety of geometrical estimates and arrangements [10]. The influences of very small-scale interactions between the neighboring material particles or constituents must be taken into account for these micro / nano-structures, such as actuators, sensors, microscopes, micro / nano-electronic systems (MEMS / NEMS). It is important for MEMS planners to understand the mechanical properties of adaptable smaller scales in order to remember the true aim of providing for the measure of diversion from associated loads to forestall cracks, improve the execution and produce the lifetime of MEMS devices [11].

From the discussion above, the principle of vibration is well-known and well-studied in dual beam systems. Nevertheless, the scale-dependent vibration of beam systems makes few contribution. The structures of scale-dependent nanobeams are constructed from nano-materials. These nanomaterials have special properties because of their dimensions of the nanoscale. Nanoparticles, nanowires and nanotubes are common examples of the materials with attractive features on the nanoscale [12].

Nanomaterials are technological products for the next century and have intensified the interest of the scientific community in physics, chemistry, biomedicine and technology. In the mechanical properties, the scale of these structures was very small, and both research and atomic reproduction measurements showed a considerable impact. In this sense, the effect of size plays a vital role in the dynamic and static conduct of micro and nanoscale structures and cannot be undermined. It is

 doi:10.20944/preprints202008.0405.v1

understood that the conventional process of the continuum in small and nanoscale systems does not have these dimensional influences. Nanomaterials are used as complex electromechanical nanostructures (NEMS) and complex nanocomposites due to some attractive properties. Nanoscale beams are referred to as structural beams constructed from nanomaterials and nanometer measurements.

The small-scale impact in the non-local elastics theory is defined by the assumption that stress at one point depends at all points on strains in the field (Eringen, [13]). It is distinct from the classical theory of elasticity. Non-local theory takes into account interatomic interaction over a long time and findings are dependent on the body size. The non-local theory includes knowledge about the long-range forces between iota along these lines, and the internal length scale is essentially used as a material parameter to detect the small scale effect. Any inconveniences of classical continuum theory can be easily eschew and the non-local elasticity theory may describe the size-dependent phenomena fairly. The use of conventional theory in studying nanostructures is inappropriate in this particular situation because classical theories are not responsible for the small-scale effects of the size.

Recent nanotechnology consideration has been given to the application of nonlocal elasticity in smaller scales and nanomaterials, and the written text indicates that the non-local elasticity principle is typically used progressively to analyze the nanostructures in a consistent and rapid manner. The fundamental contrast of conventional local theory of elasticity to Eringen's nonlocal theory of elasticity [13–15] depends on the context of the stress field. The non-local elasticity theory, however, has been applied in various material science areas, including elastic wave dispersion, mechanical decomposition, etc.

The Eringen theory of non-local elasticity has demonstrated clear theory studies of the free Vibratory of nanoparticles and nanobeams (ENET) taking into account the theories of Euler-Bernoulli (EBT) and Timoshenko beams (TBT) [16-23].

Another area of research that is emerging due to its current and future applications of various MEMS and NEMS systems is theoretical research into the behavior of rotating micro/nanobeams. Nanostructures undergoing rotation include nanostructures, nano-turbines, molecular bearings, waft and cord, and multiplicity of gear systems.

Taking into account the number of published studies of the viability of rotating nanoscale structures, this idea is expected to be given significant attention in the near future; existing samples include the analysis of molecular carbon nanotubes and gears [24, 25]. The rotational dynamics of carbon nanotubes and gears have been explained by Srivastava [26] under a single imposed laser beam. The mathematical modeling for the rotating nanomotor was carried out by Lohrasebi and Rafii-Tabar [27]. Nanoelectromechanical (NEMS) devices emerge as the next technology, which is capable of making a significant difference in people's lives.

Considering that rotating devices and rotating motors are particularly important for advancing technology, nanobeams under rotation are examined to determine their vibrational characteristics in present research. The analysis of free vibration computability of rotating beams based on classical theory, because of huge practical applications of rotating beams-like structures, has been for years an

Preprints (www.preprints.org) | NOT PEER-REVIEWED | Posted: 19 August 2020 doi:10.20944/preprints202008.0405.v1

interesting and challenging question. Some of these important studies are conducted with homogenous rotating beam materials [28–36].

The purpose of this work is to investigate the vibration behavior of rotating isotropic nanobeams in a mathematical model using Eringen's nonlocal theory of elasticity. Since the rotating devices and rotary engines are of particular importance to such advanced technology, the vibration characteristics of rotating nanobeams are investigated in current work. The model can study rotatory nanobeam's axial vibration. The model is based on the beam theory of Euler-Bernoulli, generalized dual phase-lag heat conduction and incorporates spin-smoothing and Coriolis influences. The Hamilton's principle is used to derive system equations including virtual displacements. For the first time ever the current advanced nano-rotating model is reported. This study would contribute to a complete understanding of the dynamics of rotating nanobeams. The effects due to the non-local parameter, point load, rotational and angular frequency of the thermal vibration will be taken into account. Moreover, numerical results are shown to indicate the slight effect of the nanobeam on the resonator.

2. Nonlocal model of thermoelasticity

Eringen [13] proposed a non-local continuum mechanics theory to study the structural problems at a micro-scale. For nano-scale beams the general equations of nonlocal constituent relations can be described as follows [14].

$$[1-(e_0 a)^2\nabla^2]\tau_{kl} = \sigma_{kl}, \tag{1}$$

where $\boldsymbol{\tau_{kl}}$ *denotes the nonlocal tensor stress,* $\boldsymbol{\sigma_{kl}}$ *denotes to the classical stress tensor,* $\boldsymbol{\nabla^2}$ *refers to the Laplacian,* $\boldsymbol{a}$ *is the internal trademark length,* $\boldsymbol{l}$ *is the external trademark length and* $\boldsymbol{e_0}$ *is a constant suitable to every material. The classical elasticity equation would be reached if the parameter* $\boldsymbol{a}$ *is supposed to be zero (*$\boldsymbol{e_0 a = 0}$*).*

The constitutive equation is expressed as

$$\sigma_{ij} = 2\mu e_{ij} + [\lambda e_{kk} - \gamma(T-T_0)]\delta_{ij}, \tag{2}$$

Where λ and μ are the Lame' constants and δ_{ij} refers to the function of Kronecker's delta. If $\theta = T - T_0$ is the temperature increment over the uniform reference temperature T_0 and $e = \operatorname{div}\vec{u}$ is the volumetric strain.

The modified heat conduction equation that includes two phase delay will be follows [2-4]

$$\left(1+\tau_\theta\frac{\partial}{\partial t}\right)\left(K\theta_{,i}\right)_{,i} = \left(1+\tau_q\frac{\partial}{\partial t}+\frac{1}{2}\tau_q^2\frac{\partial^2}{\partial t^2}\right)\left(\rho C_E\frac{\partial\theta}{\partial t}+\gamma T_0\frac{\partial e}{\partial t}-\rho Q\right), \tag{3}$$

Where Q is the heat source $\gamma = E\alpha_T/(1-2\nu)$, where α_T is the thermal expansion coefficient, E is the module of Young and ν is the ratio of Poisson, K implies the thermal conductivity, C_E denotes the specific heat for each unit mass and ρ is the material density.

The theory of classical thermoelasticity, the Lord and Shulman model [1], and dual-phase-delay model [2-4] can be derived from Eq. (3) for the selection of different phase lag parameters τ_θ and τ_q.

Preprints (www.preprints.org) | NOT PEER-REVIEWED | Posted: 19 August 2020 doi:10.20944/preprints202008.0405.v1

- By putting $\tau_\theta = \tau_q = 0$ in Eq. (3), we get the nonlocal theory of the coupled thermoelasticity (CTE).
- The generalized theory of nonlocal thermoelasticity (LS theory) can be gotten after placing $\tau_\theta = 0$ and $\tau_q = \tau_0$ (τ_0 is the relaxation time).
- The nonlocal dual-phase-lag model (DPL) can be obtained by setting $0 < \tau_\theta \leq \tau_q$.

When one of the thermo-physical characteristics (K, C_E and ρ) is based on temperature, Eq. (3) is converted to a nonlinear partial differential equation.

$$\lambda = \frac{E\nu}{(1+\nu)(1-2\nu)}, \quad \mu = \frac{E}{2(1+\nu)}. \tag{4}$$

3. Problem formulation

Figure 1 displays a schematic diagram of a thermoelastic rotating nanoscale beam. The length L, width b and thickness h are the geometric dimensions of the nanoscale beam. The x-axis is taken around the pivot of the nanobeam and its width and thickness are the y- and z-axes. Initially, we assume that the nanobeam is unrestricted and uncompressed and the temperature is tentatively at T_0. Under the Euler-Bernoulli principle, every plane cross-section perpendicular to the nanobeam pivot, in the beginning, is plane and perpendicular to the unbiased surface. The displacements can, therefore, be expressed as

$$u = -z\frac{\partial w}{\partial x}, \quad v = 0, \quad w = w(x,t), \tag{5}$$

where w denotes the nanobeam deflection.

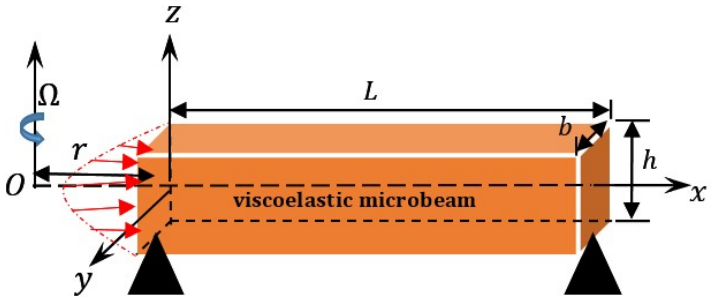

Fig. 1: Schematic chart for the nanobeam.

Equation (5) can be used to simplify the one dimension constitutive relationship (1) as

$$\sigma_x - \xi\frac{\partial^2\sigma_x}{\partial x^2} = -E\left(z\frac{\partial^2 w}{\partial x^2} + \alpha_T\theta\right), \tag{6}$$

where σ_x indicates the nonlocal axial thermal stress, $\alpha_T = \alpha_t/(1-2\nu)$ and $\xi = (e_0 a)^2$. The bending moment of the nanobeam may be found from the following integration:

$$M(x,t) = \int_{-h/2}^{h/2} z\sigma_x \mathrm{d}z. \tag{7}$$

Preprints (www.preprints.org) | NOT PEER-REVIEWED | Posted: 19 August 2020 doi:10.20944/preprints202008.0405.v1

We can get the following partial differential equation satisfied by the bending moment after substituting Eq. (6) in Eq. (7)

$$M(x,t) - \xi \frac{\partial^2 M}{\partial x^2} = -EI\left(\frac{\partial^2 w}{\partial x^2} + \alpha_T M_T\right), \tag{8}$$

where EI and $I = bh^3/12$ respectively represent the bending rigidity of the nanobeam and the inertia moment of the cross-section. In Eq. (8) M_T indicates the thermal moment of nanobeam which is given by

$$M_T = \frac{12}{h^3}\int_{-h/2}^{h/2} \theta(x,z,t) z \mathrm{d}z. \tag{9}$$

It is assumed that the nanoscale beam distributed by a transversely varying load $q(x,t)$, then the transverse motion equation can be written as [37]

$$\frac{\partial^2 M}{\partial x^2} = -q(x,t) + \rho bh \frac{\partial^2 w}{\partial t^2}, \tag{10}$$

We suppose that the nanobeam rotates about an axis parallel to the z-axis with an angular velocity Ω centered at a small distance r from the first edge of the nanobeam. The centrifugal tensional force $R(x)$ is introduced as a result of rotation. In this case, the equation of transverse motion (10) can be expressed as [37]

$$\frac{\partial^2 M}{\partial x^2} + \frac{\partial}{\partial x}\left(R(x)\frac{\partial w}{\partial x}\right) + q(x,t) = \rho bh \frac{\partial^2 w}{\partial t^2} \tag{18}$$

If $\Omega = 0$; i.e., there is no rotation and therefore the centrifugal tension force R disappears.

The axial force $R(x)$ due to centrifugal stiffening at a distance x from the origin (Fig. 1) is is given as [37, 38]

$$R(x) = \int_x^L \rho A \Omega^2 (r + x) dx \tag{19}$$

The constant r is the distance from the rotation center to the first edge of the nanobeam (a hub radius) (see Figure 1). After integration, then Eq. (19) can be simplified as

$$\begin{aligned} R(x) &= \frac{\rho A \Omega^2}{2}[(L+r)^2 - (L+x)^2] \\ &= \frac{\rho A \Omega^2}{2}[(r-x)(2L+r+x)] \end{aligned} \tag{20}$$

For calculating the bending moment $M(x,t)$, Eqs. (16) and (18) can be used

$$M(x,t) = \xi\left(\rho A \frac{\partial^2 w}{\partial t^2} - q(x,t) - \frac{\partial}{\partial x}\left(R(x)\frac{\partial w}{\partial x}\right)\right) - EI\left(\frac{\partial^2 w}{\partial x^2} + \alpha_T M_T\right) \tag{21}$$

If the moment M is removed from Eqs. (18) and (21), the equation of motion (66) may be written as

$$\left[\frac{\partial^4}{\partial x^4} + \frac{\rho A}{EI}\frac{\partial^2}{\partial t^2}\left(1 - \xi\frac{\partial^2}{\partial x^2}\right)\right] w - \frac{1}{EI}\left(1 - \xi\frac{\partial^2}{\partial x^2}\right)\left[q + \frac{\partial}{\partial x}\left(R(x)\frac{\partial w}{\partial x}\right)\right] + \alpha_T \frac{\partial^2 M_T}{\partial x^2} = 0 \tag{22}$$

The modified heat conduction equation (11) is given in the absence of heat sources $(Q = 0)$ as

$$\left(1 + \tau_\theta \frac{\partial}{\partial t}\right)\nabla.(K_x \nabla\theta) = \left(1 + \tau_q \frac{\partial}{\partial t} + \frac{\tau_q^2}{2}\frac{\partial^2}{\partial t^2}\right)\frac{\partial}{\partial t}\left(\rho C_E \theta - \gamma T_0 z \frac{\partial^2 w}{\partial x^2}\right) \tag{23}$$

Preprints (www.preprints.org) | NOT PEER-REVIEWED | Posted: 19 August 2020 doi:10.20944/preprints202008.0405.v1

4. Thermal properties of materials

The identification and resolution of nonlinear problems will be carried out if the material is temperature-dependent and then the specific heat C_E and the thermal conductivity K depends upon the temperature distribution [24]. In this work, it can be assumed that other physical parameters are constant and not dependent on temperatures, such as the Poisson's ratio and the thermal expansion coefficient [39]. The material's thermal conductivity K will be assumed to be a linear function of the variation of the temperature θ [13] as

$$K_x = K_x(\theta) = K_0(1 + K_1\theta), \tag{13}$$

Where the parameter K_0 denotes the thermal conductivity at $T = T_0$ and K_1 is a factor that characterizes thermal conductivity variety.

By substituting from equation (13) in equation (20), we obtain a partial nonlinear differential equation in the form

$$K_0\left(1 + \tau_\theta \frac{\partial}{\partial t}\right)\nabla.\left((1 + K_1\theta)\nabla\theta\right) = \left(1 + \tau_q \frac{\partial}{\partial t} + \frac{\tau_q^2}{2}\frac{\partial^2}{\partial t^2}\right)\frac{\partial}{\partial t}\left(\rho C_E\theta - \gamma T_0 z\frac{\partial^2 w}{\partial x^2}\right) \tag{23}$$

The previous equation can be converted to a linear equation by defining the mapping [40]

$$K_0\psi = \int_0^\theta K_x(\theta)\mathrm{d}\theta, \tag{14}$$

After inserting Eq. (13) in Eq. (14) and integration, then we have [40]

$$\psi = \theta\left(1 + \tfrac{1}{2}K_1\theta\right). \tag{15}$$

Through differentiating relation 5 once with regard to distances and also in terms of time, the following relationships can be deduced

$$\nabla\psi = \frac{K_r(\theta)}{K_0}\nabla\theta, \tag{16}$$

$$\frac{\partial\psi}{\partial t} = \frac{K_r(\theta)}{K_0}\frac{\partial\theta}{\partial t}. \tag{17}$$

By using Eqs. (16) and (17) then, the heat conduction equation (23) may be reduced to

$$\left(1 + \tau_\theta \frac{\partial}{\partial t}\right)\left(\frac{\partial^2}{\partial x^2} + \frac{\partial^2}{\partial z^2}\right)\psi = \left(1 + \tau_q \frac{\partial}{\partial t} + \tfrac{1}{2}\tau_q^2\frac{\partial^2}{\partial t^2}\right)\frac{\partial}{\partial t}\left(\eta\psi - \frac{\gamma T_0}{K}z\frac{\partial^2 w}{\partial x^2}\right). \tag{19}$$

where $1/\eta = K/\rho C_E$ is the thermal diffusivity.

5. Sinusoidal solution

To solve the problem, we take the temperature change solution as (sinusoidal solution).

$$\{\psi, \theta\}(x, z, t) = \{\Psi, \Theta\}(x, t)\sin\left(\frac{\pi}{h}z\right). \tag{20}$$

Presenting Eq. (20) into Eqs. (11), (12) and (19), leads to

$$\left[\frac{\partial^4}{\partial x^4} + \frac{\rho A}{EI}\frac{\partial^2}{\partial t^2}\left(1 - \xi\frac{\partial^2}{\partial x^2}\right)\right]w - \frac{1}{EI}\left(1 - \xi\frac{\partial^2}{\partial x^2}\right)q + \frac{24\alpha_T}{\pi^2 h}\frac{\partial^2\Psi}{\partial x^2} = 0, \tag{21}$$

Preprints (www.preprints.org) | NOT PEER-REVIEWED | Posted: 19 August 2020 doi:10.20944/preprints202008.0405.v1

$$M(x,t) = \xi\left(\rho A\frac{\partial^2 w}{\partial t^2} - q\right) - EI\left(\frac{\partial^2 w}{\partial x^2} + \frac{24T_0\alpha_T}{\pi^2 h}\Theta\right), \tag{22}$$

$$\left(1+\tau_\theta\frac{\partial}{\partial t}\right)\left(\frac{\partial^2}{\partial x^2} - \frac{\pi^2}{h^2}\right)\Psi = \left(1+\tau_q\frac{\partial}{\partial t} + \frac{1}{2}\tau_q^2\frac{\partial^2}{\partial t^2}\right)\frac{\partial}{\partial t}\left(\eta\Psi - \frac{\gamma T_0\pi^2 h}{24K}\frac{\partial^2 w}{\partial x^2}\right). \tag{23}$$

The following non-dimensional variables are provided for convenience.

$$\begin{gathered}\{u', x', L', w', z', h', b'\} = \eta c\{u, x, L, w, z, h, b\}, \quad \left\{t', \tau_q', \tau_\theta'\right\} = \eta c^2\left\{t, \tau_q, \tau_\theta\right\}, \\ \xi' = \eta^2 c^2\xi, \quad \{\Theta', \Psi'\} = \frac{1}{T_0}\{\Theta, \Psi\}, \quad M' = \frac{1}{\eta cEI}M, \quad q' = \frac{A}{EI}q, \quad c^2 = \frac{E}{\rho}.\end{gathered} \tag{24}$$

After introducing dimensionless quantities (24) in Eqs. (21)-(23), we can obtain

$$\left[\frac{\partial^4}{\partial x^4} + \frac{12}{h^2}\frac{\partial^2}{\partial t^2}\left(1 - \xi\frac{\partial^2}{\partial x^2}\right)\right]w - \left(1 - \xi\frac{\partial^2}{\partial x^2}\right)\left[q + \frac{\partial}{\partial x}\left(R(x)\frac{\partial w}{\partial x}\right)\right] + \frac{24T_0\alpha_T}{\pi^2 h}\frac{\partial^2\Theta}{\partial x^2} = 0 \tag{29}$$

$$\left(1+\tau_\theta\frac{\partial}{\partial t}\right)\left(\frac{\partial^2}{\partial x^2} - \frac{\pi^2}{h^2}\right)\Psi = \left(1+\tau_q\frac{\partial}{\partial t} + \frac{\tau_q^2}{2}\frac{\partial^2}{\partial t^2}\right)\frac{\partial}{\partial t}\left(\Psi - \frac{\gamma\pi^2 h}{24K\eta}\frac{\partial^2 w}{\partial x^2}\right) \tag{30}$$

$$M(x,t) = \frac{12\xi}{h^2}\frac{\partial^2 w}{\partial t^2} - \xi\left[q + \frac{\partial}{\partial x}\left(R(x)\frac{\partial w}{\partial x}\right)\right] - \frac{\partial^2 w}{\partial x^2} - \frac{24T_0\alpha_T}{\pi^2 h}\Theta \tag{31}$$

In Eqs. (29)-(31), the primes are omitted for convenience

Special external transverse load type is now taken into account. We consider exponential time of decay to vary vertically load operating towards the thickness of the beam [41].

$$q(x,t) = -q_0\left(1 - \delta e^{-\beta t}\right) \tag{32}$$

where q_0 is the magnitude of the dimensionless point load and β is the dimensionless decaying parameter of the applied load, respectively ($\delta = 0$ for the uniformly distributed load).

In this paper, we assume that the nanobeam rotates at a constant angular speed, and consider the centrifugal tension force $R(x)$ to be the maximum [37] value. The maximum axial force $R(x)$ due to centrifugal stiffening at the root ($x = 0$) takes the form [37]

$$R_{max} = \int_0^L \rho A\Omega^2(r+x)dx = \frac{1}{2}\rho A\Omega^2 L(2r+L) \tag{33}$$

The motion equation (29) is therefore can be described as

$$\left[\frac{\partial^4}{\partial x^4} + \frac{12}{h^2}\frac{\partial^2}{\partial t^2}\left(1 - \xi\frac{\partial^2}{\partial x^2}\right)\right]w - \left(1 - \xi\frac{\partial^2}{\partial x^2}\right)\left[q + \frac{6L\Omega^2(2r+L)}{h^2}\frac{\partial^2 w}{\partial x^2}\right] + \frac{24T_0\alpha_T}{\pi^2 h}\frac{\partial^2\Theta}{\partial x^2} = 0 \tag{34}$$

The bending moment in Eq. (31) may also be defined as

$$M(x,t) = \frac{12\xi}{h^2}\frac{\partial^2 w}{\partial t^2} - \xi\left[q + \frac{6L\Omega^2(2r+L)}{h^2}\frac{\partial^2 w}{\partial x^2}\right] - \frac{\partial^2 w}{\partial x^2} - \frac{24T_0\alpha_T}{\pi^2 h}\Theta \tag{35}$$

6. Initial and boundary conditions

The initial conditions are supposed to be

$$\Psi(x,0) = \frac{\partial\Psi(x,0)}{\partial t} = 0, \quad w(x,0) = \frac{\partial w(x,0)}{\partial t} = 0. \tag{29}$$

Preprints (www.preprints.org) | NOT PEER-REVIEWED | Posted: 19 August 2020 doi:10.20944/preprints202008.0405.v1

The nanobeam fulfill the following boundary conditions:

i) Clamped–clamped boundary conditions

$$w(x,t)|_{x=0,L} = 0, \quad \left.\frac{\partial w(x,t)}{\partial x}\right|_{x=0,L} = 0. \tag{30}$$

ii) The nanobeam is harmonically heated as

$$\Theta(0,t) = \Theta_0 \cos(\omega t), \quad \omega > 0, \tag{31}$$

Where Θ_0 is constant and ω is the thermal vibration angular frequency. The problem will thermal shock if by taking $\omega = 0$.

Using Eqs. (15) in equation (20), we get

$$\Psi(0,t) = \Theta_0 \cos(\omega t) + \tfrac{1}{2} K_1 [\Theta_0 \cos(\omega t)]^2. \tag{32}$$

iii) in the surface $x = L$

$$\frac{\partial \Psi(L,t)}{\partial x} = 0. \tag{33}$$

7. Laplace transform strategy

Using Laplace technique, the equations (30), (34) and (35) are converted to equations.

$$\left[\left(1 + \frac{6\xi L\Omega^2(2r+L)}{h^2}\right)\frac{\mathrm{d}^4}{\mathrm{d}x^4} - \left(\frac{12\xi s^2}{h^2} + \frac{6L\Omega^2(2r+L)}{h^2}\right)\frac{\mathrm{d}^2}{\mathrm{d}x^2} + \frac{12s^2}{h^2}\right]\bar{w} = -\frac{24T_0\alpha_T}{\pi^2 h}\frac{\mathrm{d}^2\bar{\Theta}}{\mathrm{d}x^2} - \bar{g}(s) \tag{41}$$

$$(1+\tau_\theta s)\left(\frac{\mathrm{d}^2}{\mathrm{d}x^2} - \frac{\pi^2}{h^2}\right)\bar{\Psi} = s\left(1 + \tau_q s + s^2\tau_q^2/2\right)\left(\bar{\Psi} - \frac{\gamma\pi^2 h}{24K\eta}\frac{\mathrm{d}^2\bar{w}}{\mathrm{d}x^2}\right) \tag{42}$$

$$\bar{M}(x,s) = \frac{12\xi s^2}{h^2}\bar{w} - \left(1 + \frac{6\xi L\Omega^2(2r+L)}{h^2}\right)\frac{\mathrm{d}^2\bar{w}}{\mathrm{d}x^2} - \frac{24T_0\alpha_T}{\pi^2 h}\bar{\Theta} - \xi\bar{g}(s) \tag{43}$$

Where $\bar{g}(s) = q_0\left(\frac{1}{s} - \frac{\delta}{\beta+s}\right)$.

The following differential equation can be accomplished once the function $\bar{\Theta}$ has been extracted from the Eqs. (41) and (42)

$$\left[\frac{\mathrm{d}^6}{\mathrm{d}x^6} - A\frac{\mathrm{d}^4}{\mathrm{d}x^4} + B\frac{\mathrm{d}^2}{\mathrm{d}x^2} - C\right]\bar{w} = A_5\bar{g}(s)/A_1 \tag{44}$$

where

$$\begin{aligned} &A = \frac{1}{A_1}(A_5A_1 + A_2 + A_4A_6), \quad B = \frac{1}{A_1}(A_5A_2 + A_3), \quad C = \frac{A_5A_3}{A_1}, \\ &A_1 = \left(1 + \frac{6\xi L\Omega^2(2r+L)}{h^2}\right), \; A_2 = \left(\frac{12\xi s^2}{h^2} + \frac{6L\Omega^2(2r+L)}{h^2}\right), \; A_4 = \frac{24T_0\alpha_T}{\pi^2 h}, \\ &A_3 = \frac{12s^2}{h^2}, \; A_5 = \frac{\pi^2}{h^2} + \frac{s(1+\tau_q s+s^2\tau_q^2/2)}{1+\tau_\theta s}, A_6 = \frac{s(1+\tau_q s+s^2\tau_q^2/2)}{1+\tau_\theta s}\left(\frac{\gamma\pi^2 h}{24K\eta}\right). \end{aligned} \tag{45}$$

We achieve the general solution for $\bar{w}$ by solving the differential equation (44) as follows

$$\bar{w}(x,s) = \sum_{j=1}^{3}\left(C_j \mathrm{e}^{-m_j x} + C_{j+3}\mathrm{e}^{m_j x}\right) - \frac{A_5\bar{g}(s)}{CA_1} \tag{46}$$

From the given boundary conditions the undetermined parameters $C_j, (j = 1,2..,6)$, may be calculated. The parameters m_1^2, m_2^2 and m_3^2 also satisfy the following equation

Preprints (www.preprints.org) | NOT PEER-REVIEWED | Posted: 19 August 2020 doi:10.20944/preprints202008.0405.v1

$$m^6 - Am^4 + Bm^2 - C = 0 \tag{47}$$

Eq. (46) is incorporated into Eq. (41) and results in

$$\bar{\Psi}(x,s) = -\frac{1}{A_4A_5}\left[A_1\frac{\mathrm{d}^4\bar{w}}{\mathrm{d}x^4} - (A_2 + A_4A_6)\frac{\mathrm{d}^2\bar{w}}{\mathrm{d}x^2} + A_3\bar{w} + \bar{g}(s)\right] \tag{48}$$

With the help of Eq. (46), the solution of Eq. (48) can be simplified as follows

$$\bar{\Psi}(x,s) = \sum_{j=1}^{3} H_j\left(C_j\mathrm{e}^{-m_jx} + C_{j+3}\mathrm{e}^{m_jx}\right) - H_4, \tag{49}$$

where

$$H_j = -\frac{1}{A_4A_5}\left[A_1m_j^4 - (A_2 + A_4A_6)m_j^2 + A_3\right], \quad H_4 = \frac{\bar{g}(s)(A_4 - C)}{CA_4A_5} \tag{50}$$

The bending moment $\bar{M}$ is determined from (43) using the solutions (46) and (49)

$$\bar{M}(x,s) = \sum_{j=1}^{3} L_j\left(C_j\mathrm{e}^{-m_jx} + C_{j+3}\mathrm{e}^{m_jx}\right) + L_4 \tag{51}$$

where

$$L_j = -\left(A_1m_j^2 + A_4H_j - A_0\right),\ L_4 = \bar{g}(s)\left(A_4H_4 - \frac{A_0A_5}{CA_1} - \xi\right), A_0 = \frac{12\xi s^2}{h^2} \tag{52}$$

The axial displacement u can be calculated by using Eq. (46)

$$\bar{u} = -z\frac{\mathrm{d}\bar{w}}{\mathrm{d}x} = z\sum_{j=1}^{3} m_j\left(C_j\mathrm{e}^{-m_jx} - C_{j+3}\mathrm{e}^{m_jx}\right). \tag{53}$$

The boundary conditions (37)-(40) are reduced in the Laplace transform field to

$$\bar{w}(x,s)|_{x=0,L} = 0, \quad \left.\frac{\mathrm{d}^2\bar{w}(x,s)}{\mathrm{d}x^2}\right|_{x=0,L} = 0, \tag{54}$$

$$\bar{\Psi}(x,s)|_{x=0} = \Theta_0\left[\frac{s}{s^2+\omega^2} + \frac{K_1(s^2+2\omega^2)}{2s(s^2+4\omega^2)}\right] = \bar{G}(s), \tag{50}$$

$$\left.\frac{\mathrm{d}\bar{\Theta}}{\mathrm{d}x}\right|_{x=L} = 0. \tag{56}$$

When the above conditions are applied to Eqs. (46) and (49), the following system equations are given.

$$\sum_{j=1}^{3}\left(C_j + C_{j+3}\right) = \frac{A_5\bar{g}(s)}{CA_1} \tag{57}$$

$$\sum_{j=1}^{3}\left(C_j\mathrm{e}^{-m_jL} + C_{j+3}\mathrm{e}^{m_jL}\right) = \frac{A_5\bar{g}(s)}{CA_1} \tag{58}$$

$$\sum_{j=1}^{3} m_j^2\left(C_j + C_{j+3}\right) = \frac{A_5\bar{g}(s)}{CA_1} \tag{59}$$

$$\sum_{j=1}^{3} m_j^2\left(C_je^{-m_jL} + C_{j+3}e^{m_jL}\right) = \frac{A_5\bar{g}(s)}{CA_1} \tag{60}$$

$$\sum_{j=1}^{3} H_j\left(C_j + C_{j+3}\right) = H_4 + \bar{G}(s), \tag{61}$$

$$\sum_{j=1}^{3} m_jH_j\left(C_je^{-m_jL} - C_{j+3}e^{m_jL}\right) = 0, \tag{62}$$

The undetermined parameters $C_j, (j = 1,2..,6)$ can be calculated in the resolution of the above system equations.

Preprints (www.preprints.org) | NOT PEER-REVIEWED | Posted: 19 August 2020 doi:10.20944/preprints202008.0405.v1

We have thus obtained all the analytical solutions for the physical variables within the Laplace transform field. It's difficult to get the Laplace transform inversion of the complicated transformed field variables expressions. Within the next section, the results will be evaluated numerically using an expansion technique of the Fourier series.

The temperature $\bar{\theta}$ can be obtained by solving Eq. (17) after applying the Laplace transform as

$$\bar{\theta}(x,s) = \sin\left(\frac{\pi}{h}z\right)\left[\frac{-1+\sqrt{1+2K_1\bar{\psi}}}{K_1}\right] \tag{63}$$

8. Laplace transform Inversion

With the aim of getting solutions into the physical domain, at last, we invert the transformation of Laplace to the functions that govern. We now follow a numerical overlay strategy based on an extension of the Fourier series [42]. Any functions in the domain Laplace $\bar{g}(x,s)$ can be changed to the time field $g(x,t)$ in this procedure by using the relation.

$$g(x,t) = \frac{e^{ct}}{t}\left\{\frac{1}{2}\bar{g}(x,c) + \mathrm{Re}\left[\sum_{n=1}^{N}(-1)^n\,\bar{g}\left(x,c+\frac{in\pi}{t}\right)\right]\right\}, \tag{59}$$

Various numerical studies have shown that the parameter c satisfies the relation $ct \approx 4.7$ for speedier convergence [43].

9. Results and Discussion

Throughout this section, we provide some discussions and numerical results to illustrate the general solution behavior of the theoretical outcomes. In addition, numerical results are provided to determine the effects on the physical fields analyzed with three appropriate parameters. We have taken specific physical parameters from various current literature works into account for computational purposes. In this analysis, we use silicon data as the physical material discussed:

$$E = 169\ \mathrm{GPa},\quad \rho = 2330\left(\frac{\mathrm{kg}}{\mathrm{m}^3}\right),\quad C_E = 713\left(\frac{\mathrm{J}}{\mathrm{kg\ K}}\right),$$
$$\alpha_T = 2.59\times10^{-9}\left(\frac{1}{\mathrm{K}}\right),\ \nu = 0.22,\ T_0 = 293\ K,\ K = 156\left(\frac{\mathrm{W}}{\mathrm{mK}}\right).$$

We consider a nano-beam with dimensionless parameters as given in equation (24). The ratios of the nanobeam are set in the current calculation, i.e., $L/h = 10$ and $b/h = 0.5$. The dimensionless nanobeam length is taken as $L = 1$ and take $z = h/3$ and time $t = 0.1$. Three cases for discussion and analysis are considered using the nonlocal theory of Eringen.

As mentioned previous, a linear function of the variation in temperature θ is assumed to be the thermal conductivity K of the material (see Eq. (13)). That is the main goal of the analysis. Figures 2-5 show the differences in non-dimensional deflection, temperature increase, displacement and bending moment, compared to the K_1-parameter to illustrate the thermal properties of the nanobeam that vary according to temperature θ. Two different thermal conduction parameter cases will be considered. When the thermal conductivity depends on the temperature, the $K_1 = -1$ and $K_1 = -0.5$ will be used. If the thermal conductivity remains constant, the $K_1 = 0$ will be used. We shall

Preprints (www.preprints.org) | NOT PEER-REVIEWED | Posted: 19 August 2020 doi:10.20944/preprints202008.0405.v1

assume that the other parameters and affective factors are fixed in this case ($\xi = 0.01,\ \omega = 5,\ \Omega = 0.3,\ \tau_q = 0.02$ and $\tau_\theta = 0.01$).

From the figures we have noted that the variability parameter K_1 has a considerable impact on all fields that make our consideration of the variable thermal conductivity more seriously. The nanostructures can also be observed to based physically on temperatures and to increase external temperatures, results of small-scale nonlocal theories increase.

The deflection w with varying values of thermal conductivity variability parameter K_1 is shown in Figure 2. As can be shown, with the increased value of the parameter K_1, the lateral vibration w decreases. Figure 2 illustrates that the deflection distribution w that starts and ends at zero values (i.e. disappears) and meets the limit conditions of the rotating nanobeam at $x = 0$ and $x = L$. The temperature θ for variability parameter K_1 values can be seen in Figure 3. The temperature θ decreases with increasing distance x, in order to drive towards wave propagation, as shown in Figure 3. Figure 3 indicates that a decrease in the parameter K_1 increases the temperature distribution θ.

Figure 4 indicates that the displacement value decreases from 0 to 0.3 and consequently in the range 0.3 to 0.8 rises to the highest amplifications. The displacement u is going straight in the last range $0.8 \le x \le 1$ of wave propagation. It should be noted that the displacement distribution is highly influenced by the variability parameter K_1.

We also note that the rise in K_1 in Figure 5 is intended to increase the bending moment M distribution. The figures show that the effect of a change in thermal conductivity should not be disregarded [44]. The mechanical distributions of the nano beam show that the wave spreads in medium as a wave with a finite speed [45].

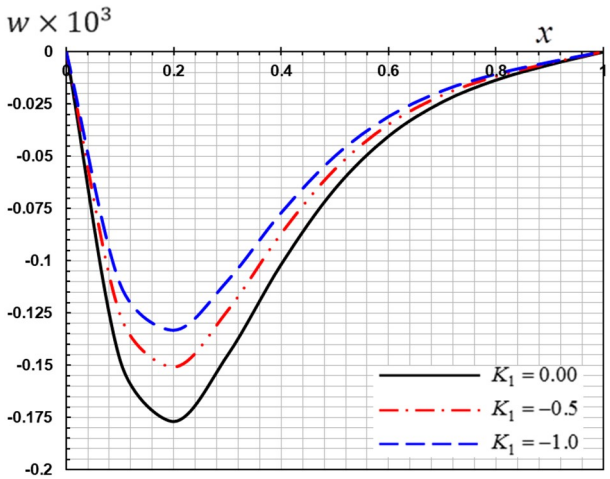

Figure 2: The deflection w under the influence of variable thermal properties

Preprints (www.preprints.org) | NOT PEER-REVIEWED | Posted: 19 August 2020 doi:10.20944/preprints202008.0405.v1

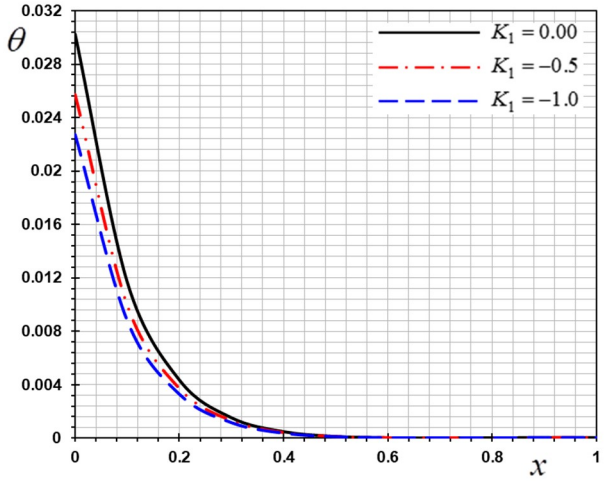

Figure 3: Temperature θ under the influence of variable thermal properties

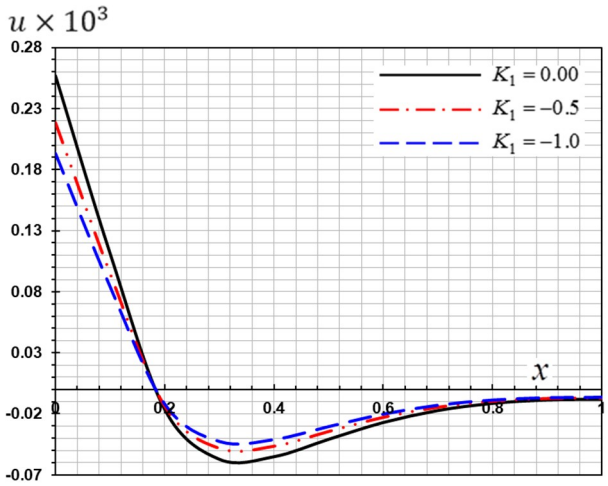

Figure 4: Displacement u under the influence of variable thermal properties

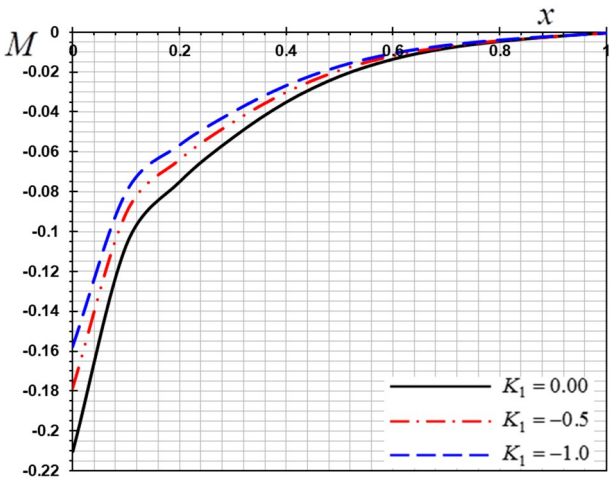

Figure 5: Bending moment M under the influence of variable thermal properties

Preprints (www.preprints.org) | NOT PEER-REVIEWED | Posted: 19 August 2020 doi:10.20944/preprints202008.0405.v1

In second case, an effect on dimensionless field quantities has been performed on the angular rotation velocity Ω. It is supposed to be consistent both the non-local parameter ξ, angular frequency of the harmonic thermal load ω, and phase lags τ_q and τ_θ. The calculations has been determined using the fixed values $\xi = 0.1$, $\omega = 5$, $\tau_q = 0.02$ and $\tau_\theta = 0.01$ have been taken into account.

The variation in the fields considered for three different values angular velocity ($\Omega = 0, 0.1, 0.3$) is shown in Figures 10-13. In the absence of rotation, the coefficient of rotation is equal to zero ($\Omega = 0$), and this is a special case in current procedure.

The angular rotation s Ω that influences the deflection of the nanoscale beam w, is shown in Figure 10. This parameter has been found to have a substantial effect on the distribution of deflection w and variation in outcomes in the case of presence and lack of rotation. Through increasing the angular velocity Ω, the deflection w decreases. These results are consistent with those reported [46].

The temperature variance θ of nanobeams with distance x was verified for different non-dimensional angular velocity values Ω. These variations are illustrated in Figures 11. Clearly, the temperature increases with the rise of the angular velocity Ω. In the previous literature the results and observations are consistent with the corresponding results obtained, as those of the authors [47, 48].

Figure 12 presents a survey of the impact of angular speed Ω on displacement variance u. We find that the curves that reflect the displacement field are influenced by the rotation. The figure shows that at certain ranges, with a rising rotation, the distribution of the displacement u decreases and increases at other intervals. Figure 13 shows the variation of varying angular velocity Ω values in the distribution of bending moment M of the rotating nanobeam. It is observed from the figure that the rotation of the moment has a great effect on the curves, and that the amplitude of the moment increases with the moment M.

One of the objectives of this analysis is to explain the approach to the temperature field and to the angular velocity of certain nano-device blades such as nano-turbines [50], which provide valuable insights. Via the previous observations, we can also deduce the major effect of rotation on the different physical distributions. The findings are in line with the earlier results of [49-51].

Preprints (www.preprints.org) | NOT PEER-REVIEWED | Posted: 19 August 2020 doi:10.20944/preprints202008.0405.v1

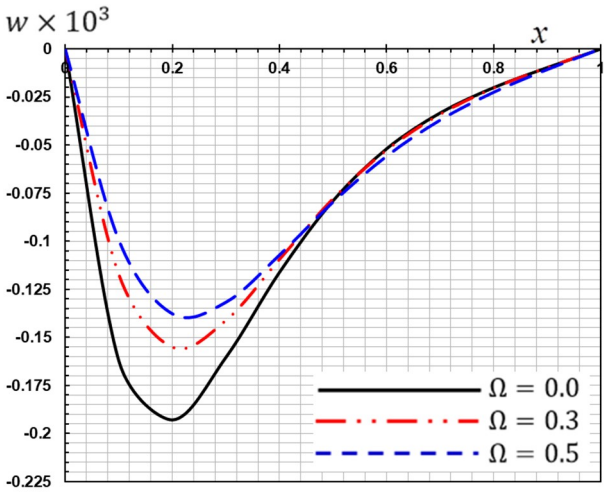

Figure 10: The deflection w via the angular velocity Ω

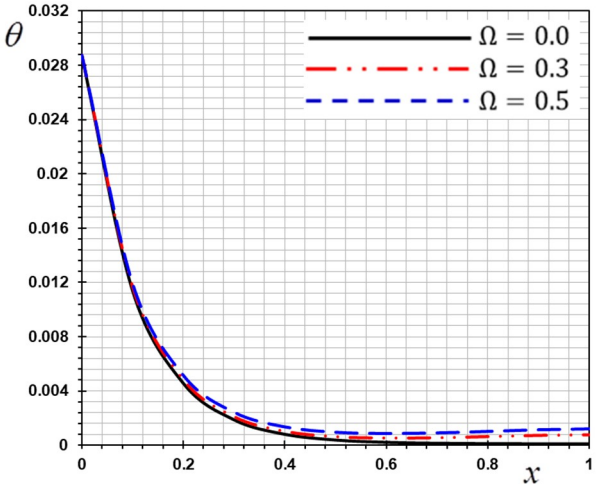

Figure 11: The temperature θ via the angular velocity Ω

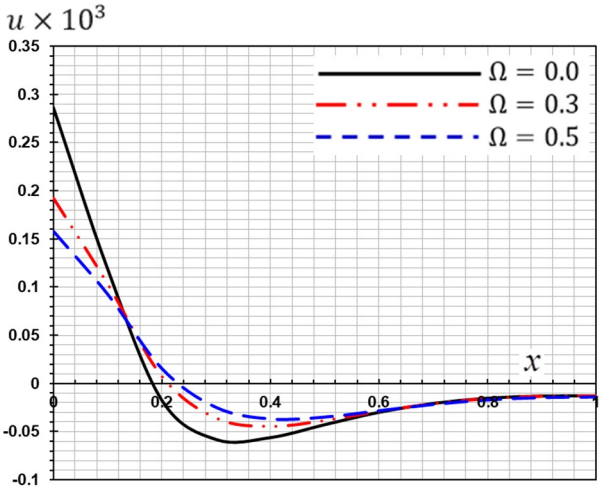

Figure 12: The displacement u via the angular velocity Ω

Preprints (www.preprints.org) | NOT PEER-REVIEWED | Posted: 19 August 2020 doi:10.20944/preprints202008.0405.v1

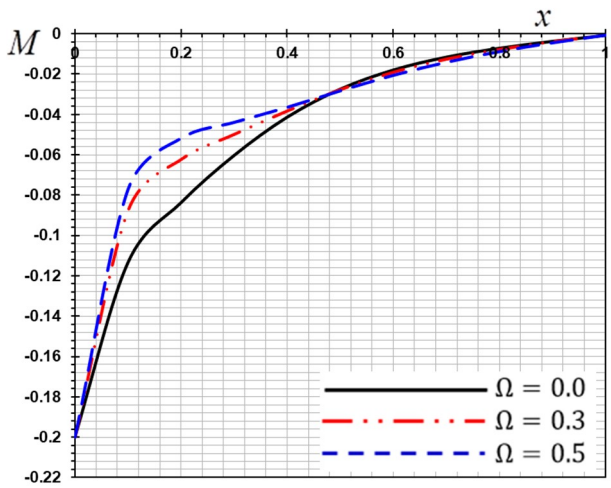

Figure 13: The bending moment M via the angular velocity Ω

When values of the parameters $(\omega, K_1, \Omega, \tau_q, \tau_\theta)$ are set, the effect of the nonlocal coefficient ξ after the non-dimensional-field, variable behavior is examined. In Figures 6-9 along the axial direction, the thermoelastic vibrations of the rotating nanobeam for different parameter values are shown. The non-local coefficient values are considered to be: $\xi = 0$ (local theory), $\xi = 0.01$ and $\xi = 0.0\,3$ for comparison. The figures indicate that local parameters influence all the fields studied. It illustrates the difference between local thermoelasticity theories and non-local ones.

For various values of the non-local scaling coefficient ξ, Figure 4 shows the curves for non-rotating nanobeam deflection. It can be seen that with an increase in the parameter of the nonlocal scaling, the deflection becomes very small and the dispersed nature turns into a non-dispersed form. The temperature distributions are also shown for the various non-local scaling parameter in the axial direction in Figure 3. The Figure shows that the temperature convergence can be accomplished by increasing the nonlocal parameter across the space. Figure 6 shows that the displacement amplitude increases with the non-local parameter due to the inclusion of the nonlocality in the given model. The influence of the non-local coefficient ξ on the distribution of the non-dimensional moment is shown in Figure 7. As the non-local coefficient ξ increases, the bending moment will decrease.

The reported findings and conclusions are consistent with those of various literature researchers [52]. The results shown typically show that the non-local parameter has a major effect on all observed physical variables. The distinction between local thermoelasticity models and non-local thermoelasticity models in thermal fields is clarified [53]. In nanoscale systems and devices the impact of this parameter should also be taken into account.

Preprints (www.preprints.org) | NOT PEER-REVIEWED | Posted: 19 August 2020 doi:10.20944/preprints202008.0405.v1

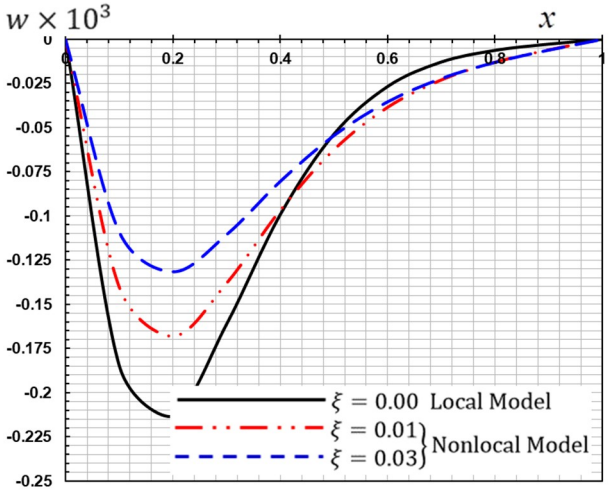

Figure 2: The deflection w distribution via the nonlocal parameter ξ

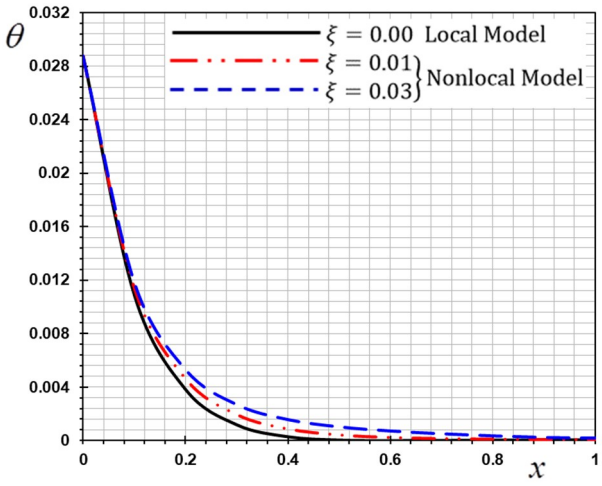

Figure 3: The temperature θ distribution via the nonlocal parameter ξ

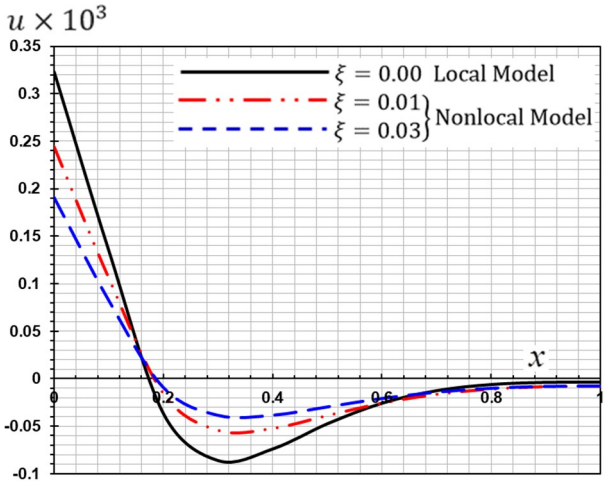

Figure 4: The isplacement u distribution via the nonlocal parameter ξ

Preprints (www.preprints.org) | NOT PEER-REVIEWED | Posted: 19 August 2020 doi:10.20944/preprints202008.0405.v1

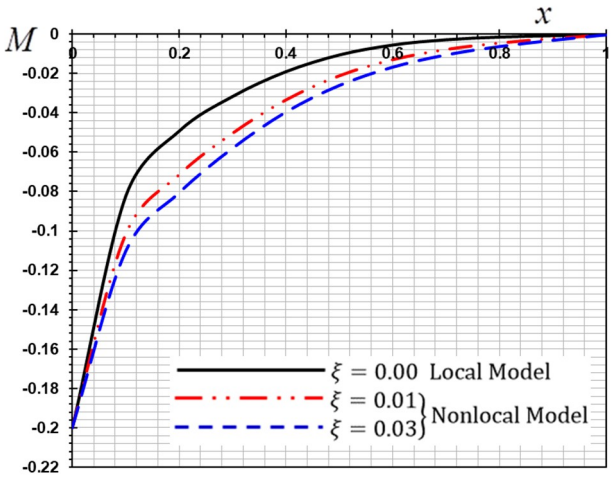

Figure 5: The bending moment M distribution via the nonlocal parameter ξ

In the last case, the variant of studied field variables studied against point load q_0 will be plotted in Figures 3. There are three different non-dimensional magnitude values for the point load q_0 that are taken into account. The figures show the point load effect. We use $\delta = 0$ for the uniformly distributed load, and we take $\delta = 1$ for the exponential decay time load. Clearly, the variations between the results become more important with a rise in the point load q_0. The figures show that the point load q_0 has a great impact on all the fields studied. Figure 6 indicates that there is a greater disparity between physical quantities with the point load in the highest points of the figures.

We also note from these figures that the absolute values of the field variables increase with the magnitude of point load q_0 if the varying load exponential decay with time [54].

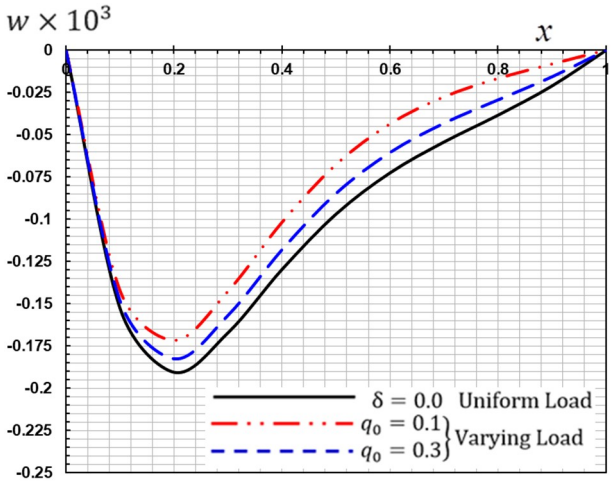

Figure 2: The deflection w under the influence the point load q_0

Preprints (www.preprints.org) | NOT PEER-REVIEWED | Posted: 19 August 2020 doi:10.20944/preprints202008.0405.v1

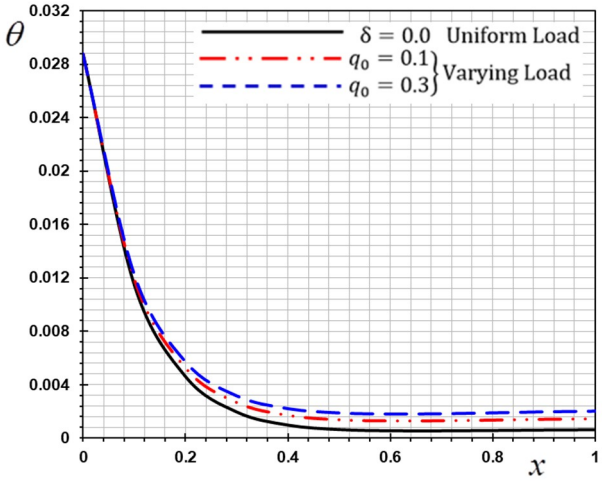

Figure 3: Temperature θ under the influence the point load q_0

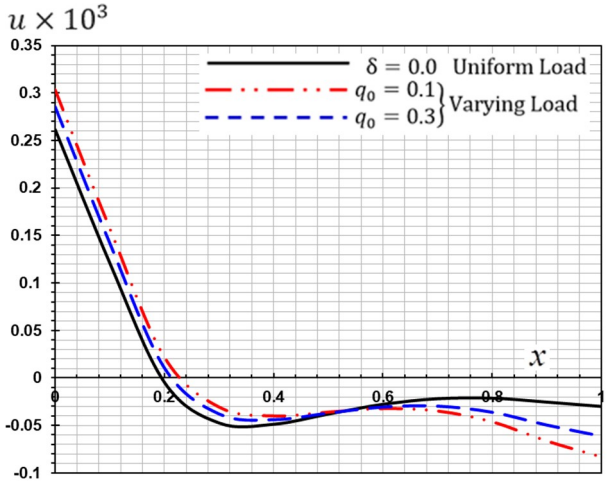

Figure 4: Displacement u under the influence of the point load q_0

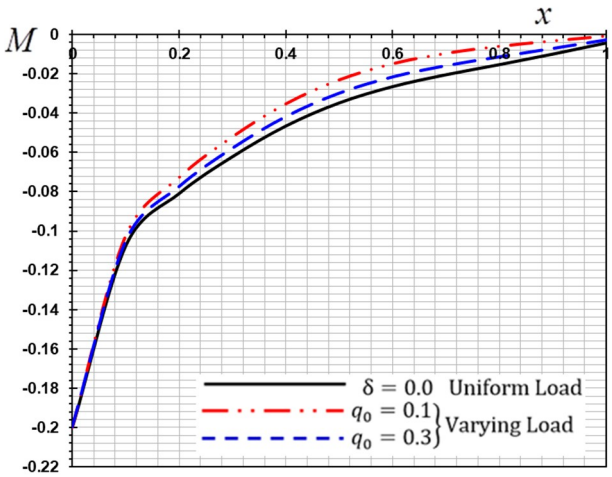

Figure 5: Bending moment M under the influence the point load q_0

 doi:10.20944/preprints202008.0405.v1

10. Conclusions

The research in this paper focuses on rotating nanobeam wave dispersion behavior using the non-local elasticity theory and generalized thermoelasticity with phase delay. The rotating beam is formed by based on the theory of Euler–Bernoulli. The thermal conductivity of the nanobeam and modulus of elasticity are considered to be temperature-dependent. For a uniform rotating nanobeam, the governing equations are derived including the variability of thermal conductivity and nonlocal scale effect. The nanobeam surface is expected to be thermally loaded with uniformly variable heat and subjected to exponential decay time load under proven boundary conditions. The dynamic load effects, the non-local variability parameter and rotation and change in thermal conductivity in the studied fields are graphically described and examined. The figures also show the following important results:

- The parameter of variation of the thermal conductivity affects the wave propagation rate of all of the fields under study. Physical fields depend strongly on thermal conductivity variability.
- The dependency from the temperature on thermal conductivity has a significant influence on mechanical and thermal interactions.
- The nonlocal parameter effects can be significant on all fields studied.
- Dynamic loads have a major impact on all physical quantities.
- There are significant variations in the fields investigated between the exponential time of decay and the load distributed uniformly. The thermoelastic stresses, and temperature, on the other hand, are highly dependent on the angular rate of the thermal vibrators parameter.
- Nanobeam research is an important subject in nanotechnology as it encompasses the optical and electronic characteristics in nanobeams.
- Current research may be used in applications including resonators, sensors for the voltage surge, frequency filters, accelerometers and relay switches.
- This study will recognize demands and various requirements for the design and production of the environmentally sensitive resonator machines.

- **Supplementary Materials:** Not applicable.
- **Author Contributions:** Writing—review and editing, both authors. Also, both authors have read and agreed to the present version of the manuscript.
- **Funding:** This work did not receive any funding.
- **Acknowledgments:** Not applicable.
- **Conflicts of Interest:** The authors declare no conflict of interest.

References

 doi:10.20944/preprints202008.0405.v1

References

1. Lord, H.W., Shulman, Y.H. A generalized dynamical theory of thermoelasticity. J. Mech. Phys. Solids, **1967**;15(5):299–309.
2. Tzou, D.Y. Thermal shock phenomena under high rate response in solids, Annual Rev. Heat Transf., **1992**, 4(4), 111–185.
3. Tzou, D.Y. A unified field approach for heat conduction from macro-to micro-scales, J. Heat Transf., **1995**, 117(1) 8–16.
4. Tzou, D.Y. The generalized lagging response in small-scale and high-rate heating," Int. J. Heat Mass Transf., **1995**, 38(17), 3231–3240.
5. Abouelregal, A.E. Two-temperature thermoelastic model without energy dissipation including higher order time-derivatives and two phase-lags. Materials Research Express, **2019**, 6(11) 116535.
6. Abouelregal, A.E. On Green and Naghdi thermoelasticity model without energy dissipation with higher order time differential and phase-lags, Journal of Applied and Computational Mechanics, **2020**, 6(3) 445–56.
7. Abouelregal, A.E. A novel generalized thermoelasticity with higher-order time-derivatives and three-phase lags", Multidiscipline Modeling in Materials and Structures, **2019** https://doi.org/10.1108/MMMS-07-2019-0138.
8. Abouelregal, A.E. Three-phase-lag thermoelastic heat conduction model with higher-order time-fractional derivatives, Indian J. Phys. **2019**, https://doi.org/10.1007/s12648-019-01635-z.
9. Berman, R . The thermal conductivity of dielectric solids at low temperatures, Advances in Physics, 2(5), (1953)103-140.
10. M.I. Younis, MEMS Linear and Non-linear Statics and Dynamics, Springer, New York, USA, **2011**.
11. Allameh, S.M. An introduction to mechanical-properties-related issues in MEMS structures, J. Mater. Sci. **2003**, 38 4115–4123.
12. Murmu, T., Adhikari, S. Nonlocal elasticity based vibration of initially pre-stressed coupled nanobeam systems, European Journal of Mechanics- A/Solids, **2012**, 34, 52-62.
13. Eringen A.C. On differential equations of nonlocal elasticity and solutions of screw dislocation and surface waves. J Appl Phys, **1983**; 54, 4703–10.
14. Eringen A.C. Nonlocal polar elastic continua. Int J Eng Sci, **1972**; 10, 1–16.
15. Eringen A.C., Edelen D.G.B. On nonlocal elasticity. Int J Eng Sci, **1972**; 10, 233–48.
16. Abouelregal, A.E., Marin, M. The size-dependent thermoelastic vibrations of nanobeams subjected to harmonic excitation and rectified sine wave heating, Mathematics **2020**; 8(7): 1128.
17. Kumar, P.R., Rao, K, M., Rao, N.M. Free vibration analysis of functionally graded rotating Beam by differential transform method. Indian Journal of Engineering and Material Sciences. **2017**, 24(2) 107-114.

18. Abouelregal, A.E., Mohammed, W.W., Effects of nonlocal thermoelasticity on nanoscale beams based on couple stress theory, Mathematical Methods in the Applied Sciences, **2020**, https://doi.org/10.1002/mma.6764.
19. Abouelregal A.E., Marin M. The response of nanobeams with temperature-dependent properties using state-space method via modified couple stress theory, Symmetry **2020**, 12(8), 1276.
20. Abouelregal, A.E., Mohamed, B.O. Fractional order thermoelasticity for a functionally graded thermoelastic nanobeam induced by a sinusoidal pulse heating, J. Comput Theor Nanosci. **2018**; 15, 1233–1242.
21. Shabani, S., Cunedioglu, Y. Free vibration analysis of cracked functionally graded non-uniform beams, Mater. Res. Express, **2020**, 7, 015707
22. Karamanl, A. Free vibration analysis of two directional functionally graded beams using a third order shear deformation theory, Compos. Struct. **2018**, 189, 127–136.
23. Lohar, H., Mitra, A., Sahoo, S. Nonlinear response of axially functionally graded Timoshenko beams on elastic foundation under harmonic excitation. Curved and Layered Structures, **2019**, 6(1), 90–104.
24. Drexler, K. E., Nanosystems: Molecular Machinery, Manufacturing, and Computation Wiley, New York, USA, **1992**.
25. Han, J., Globus, A., Jaffe, R., Deardorff, G., Molecular dynamics simulations of carbon nanotube-based gears, Nanotechnology, **1997**, 8, 95–102.
26. Srivastava, D., A phenomenological model of the rotation dynamics of carbon nanotube gears with laser electric fields, Nanotechnology, **1997**, 8, 186–192.
27. Lohrasebi, A. Rafii-Tabar, H., Computational modeling of an iondriven nanomotor, J. Mol. Graphics Modell., **2008**, 27, 116–123.
28. Yokoyama, T. Free vibration characteristics of rotating Timoshenko beams. Int J Mech Sci **1988**;30, 743–55.
29. Gunda J.B., Ganguli R. New rational interpolation functions for finite element analysis of rotating beams, Int. J. Mech. Sci., **2008**, 50, 578–88.
30. Yoo, H.H., Park, J.H., Park J. Vibration analysis of rotating pre-twisted blades, Comput. Struct. **2001**, 79(19), 1811–1819.
31. Lee, S.Y., Lin, S.M., Lin, Y.S. Instability and vibration of a rotating Timoshenko beam with precone, Int. J. Mech. Sci. **2009**; 51, 114–121.
32. Avramov, K.V., Pierre, C., Shyriaieva, N. Flexural-flexural-torsional nonlinear vibrations of pre-twisted rotating beams with asymmetric cross-sections, J. Vib. Control. **2007**, 13, 329–364.
33. Mohammadi, M., Safarabadi, M., Rastgoo, A., Farajpour, A. Hygro-mechanical vibration analysis of a rotating viscoelastic nanobeam embedded in a visco-Pasternak elastic medium and in a nonlinear thermal environment. Acta Mechanica, **2016**, 227(8), 2207–2232.
34. Faroughia, S., Rahmani, A., Friswell, M.I. On wave propagation in two-dimensional functionally graded porous rotating nano-beams using a general nonlocal higher-orderbeam model, Applied Mathematical Modelling, **2020**, 80, 169-190.

35. Ebrahimi, F., Haghi, P. Wave propagation analysis of rotating thermoelastically-actuated nanobeams based on nonlocal strain gradient theory. Acta Mechanica Solida Sinica, **2017**, 30(6), 647–657.
36. Azimi, M., Mirjavadi, S. S., Shafiei, N., Hamouda, A. M. S., Davari, E. Vibration of rotating functionally graded Timoshenko nano-beams with nonlinear thermal distribution. Mechanics of Advanced Materials and Structures, **2017**, 25(6), 467–480.
37. Narendar, S., Gopalakrishnan, S. Nonlocal wave propagation in rotating nanotube, Results in Physics, **2011**, 1, 17–25
38. Ebrahimi, F., Dabbagh, A. Wave dispersion characteristics of rotating heterogeneous magneto-electro-elastic nanobeams based on nonlocal strain gradient elasticity theory, J. Electromag. Waves Appl. **2018**, 32(2):138-169.
39. Noda, N. Thermal stress in material with temperature dependent properties, In: Thermal stresses, R.B. Hetnarski (ed), Elsevier Science, North Holland, Amsterdam, 391-483, **1986**.
40. R. Berman, The thermal conductivity of dielectric solids at low temperatures, Advances in Physics, **1953**, 2(5), 103-140.
41. Sharma, J.N., Kaur, R. Response of anisotropic thermoelastic micro-beam resonators under dynamic loads, Applied Mathematical Modelling, **2015**, 39, 2929–2941.
42. Honig, G., Hirdes, U. A method for the numerical inversion of Laplace Transform, J. Comp. Appl. Math., **1984**, 10, 113-132.
43. Tzou, D.Y. Experimental support for the lagging behavior in heat propagation, J. Thermophys. Heat Transf. **1995**, 9(4), 686–693.
44. Wang, Y., Liu, D. Wang, Q., Zhou, J. Asymptotic solutions for generalized thermoelasticity with variable thermal material properties, *Archives of Mechanics*, **2016**, 68(3), 181–202.
45. Abo-Dahab, S.M., Abouelregal, A.E., Ahmad, H. Fractional heat conduction model with phase lags for a half-space with thermal conductivity and temperature dependent. Mathematical Methods in the Applied Sciences, **2020**, doi:10.1002/mma.6614
46. Ebrahimi, F. Haghi, P. Elastic wave dispersion modelling within rotating functionally graded nanobeams in thermal environment, Advances in Nano Research, **2018**, 6(3), 201-217.
47. Shafiei, N., Kazemi, M., Ghadiri, M. Comparison of modeling of the rotating tapered axially functionally graded Timoshenko and Euler–Bernoulli microbeams. Physica E: Lowdimensional Systems and Nanostructures, **2016**, 83, 74-87.
48. Younesian, D., Esmailzadeh, E. Vibration suppression of rotating beams using timevarying internal tensile force, Journal of Sound and Vibration, **2011**, 330(2), 308-320.
49. Khaniki, H.B. Vibration analysis of rotating nanobeam systems using Eringen's two-phase local/nonlocal model. Physica E: Low-Dimensional Systems and Nanostructures, **2018**, 99, 310–319.
50. Safarabadi, M., Mohammadi, M., Farajpour, A., Goodarz, M. Effect of Surface Energy on the Vibration Analysis of Rotating Nanobeam, Journal of Solid Mechanics, **2015**, 7(3) 299-311.
51. Fang, J., Gu,J., Wang, H. Size-dependent three-dimensional free vibration of rotating functionally graded microbeams based on a modified couple stress theory, International Journal of Mechanical Sciences, **2018**, 136, 188-199.
52. Abouelregal, A.E. A novel model of nonlocal thermoelasticity with time derivatives of higher order. Mathematical Methods in the Applied Sciences, **2020** doi:10.1002/mma.6416.

53. Borjalilou, V., Asghari, M., Taati, E. Thermoelastic damping in nonlocal nanobeams considering dual-phase-lagging effect. Journal of Vibration and Control, **2020**, 26(11–12) 1042–1053.
54. Abouelregal, A.E., Zenkour, A.M. Thermoelastic response of nanobeam resonators subjected to exponential decaying time varying load, Journal of Theoretical and Applied Mechanics, **2017**, 55, 3, 937-948, Warsaw.